Published in final edited form as:
Angew Chem Int Ed Engl. 2014 October 6; 53(41): 10945–10948. doi:10.1002/anie.201406216.

Cell-Mediated Assembly of Phototherapeutics

Weston J. Smith, **Nathan P. Oien**, **Robert M. Hughes**, **Christina M. Marvin**, **Zachary L. Rodgers**, **Junghyun Lee**, and **David S. Lawrence**
Department of Chemistry, Division of Chemical Biology andMedicinal Chemistry, and Department of Pharmacology University of North Carolina, Chapel Hill, NC 27599 (USA)

David S. Lawrence: lawrencd@email.unc.edu

Abstract

Light-activatable drugs offer the promise of controlled release with exquisite temporal and spatial resolution. However, light sensitive pro-drugs are typically converted to their active forms using short wavelengths, which display poor tissue penetrance. We report herein erythrocyte-mediated assembly of long wavelength-sensitive phototherapeutics. The activating wavelength of the constructs is readily pre-assigned by using fluorophores with the desired λ_{ex}. Drug release from the erythrocyte carrier was confirmed by standard analytical tools and by the expected biological consequences of the liberated drugs in cell culture: methotrexate, binding to intracellular dihydrofolate reductase; colchicine, inhibition of microtubule polymerization; dexamethasone, induced nuclear migration of the glucocorticoid receptor.

Keywords

Photochemistry; Drug Delivery; Cobalamins; Pro-drugs

The use of light to activate therapeutic agents at disease sites offers the advantage of aggressive treatment with exquisite spatial control, thereby reducing potential deleterious side effects at unintended sites. An excellent example of this concept is photodynamic therapy, which employs the delivery of a photosensitizer to the tissue of interest.[1] Upon excitation with the appropriate wavelength of light and, in the presence of oxygen, cytotoxic reactive oxygen species are generated, resulting in destruction of the target cells. This minimally invasive procedure furnishes control over where and when the reactive oxygen species are produced. However, a more general strategy that can control the delivery of any drug could profoundly influence the treatment of a variety of disorders, including cancer, diabetes, and autoimmune and vascular diseases. A major challenge in this regard is the so-called “optical window of tissue”, the wavelength of light that enjoys maximal tissue penetration, which lies in the range of 600 – 900 nm.[2] Wavelengths less than <600 nm are absorbed by hemoglobin in the circulatory system and melanin in the skin whereas water interferes with light penetrance >900 nm. Unfortunately, nearly all light-activatable pro-drugs described to date respond to short wavelengths <450 nm.[3] This limitation is

Correspondence to: David S. Lawrence, lawrencd@email.unc.edu.
Supportinginformationforthisarticleisgiven via a link at the end of thedocument.((Pleasedeletethistextif not appropriate))

responsible for the intense interest in two-photon[4] and up converting[5] technologies. However, as discussed in recent reviews,[4–5] both technologies must overcome daunting challenges before potential therapeutic applications are realized. We recently described the long wavelength (>600 nm) photolysis of alkylcobalamins (alkyl-Cbl).[6] We now report the cell-mediated assembly of lipid-Cbl-drug and lipid-fluorophore conjugates in which the latter serve as long wavelength-capturing antennas that promote drug release.

Erythrocytes have been called the “champions of drug delivery” due to their biocompatibility, their long life span (120 days), and their size, which allows large quantities of drug to be conveyed relative to other carriers.[7] However, “practically useful controlled release from carrier RBC (red blood cells) remains an elusive goal”.[7] Our strategy to address this issue is depicted in Figure 1. Based on a previously demonstrated energy transfer between fluorophores and Cbls in covalently appended Cbl-fluorophore conjugates,[6] we decided to explore the premise that the cell-mediated assembly of C_{18}-Cbl-drug and C_{18}-fluorophore conjugates could act in concert as a photo-responsive drug delivery system. Illumination of the fluorophore antenna at its λ_{max} and subsequent energy transfer to the Cbl-drug moiety should result in cleavage of the weak Co-C bond,[6,8] thereby liberating the drug.

A series of lipidated-Cbl (C_{18}-Cbl) and C_{18}–fluorophore derivatives were prepared (Figure 2, SI Figures S1–S4, Tables S3–S6 and Scheme S1). In the case of the Cbl derivatives, the C_{18} moiety was appended to the 5 ribose –OH of Cbl using octadecylamine and carbonyl-di-triazole. Subsequent alkylation of the Co furnished an amine or carboxylic acid handle, upon which drugs and fluorescent reporters were covalently attached (Figure 2, SI Figure S5 and Schemes S2 – S7). These species include the anti-inflammatories methotrexate (MTX), colchicine (COL), and dexamethasone (DEX), and the fluorescent reporters tetramethylrhodamine (TAM) and fluorescein (FAM). The C_{18}–fluorophore derivatives were prepared via direct condensation of the activated carboxylate of the fluorophore with the amine of octadecylamine (SI Schemes S8 – S10).

Our initial studies sought to explore the premise of the Figure 1 strategy by establishing light-triggered movement of drugs and reporters from a hydrophobic environment to an aqueous one. For these preliminary experiments we directly photolyzed C_{18}-Cbl-drug and C_{18}-Cbl-reporter conjugates at the Cbl absorbance wavelength (525 nm). As expected, both **C_{18}-Cbl-TAM** and **C_{18}-Cbl-MTX** are soluble in octanol. Illumination at 525 nm cleaved the **C_{18}-Cbl-TAM** Co-C bond and promoted migration of TAM from octanol to water as assessed by fluorescence (SI Figure S6). In an analogous fashion, 525 nm illumination of **C_{18}-Cbl-MTX** triggered the release of MTX into the aqueous phase as demonstrated by LC-MS (SI Figure S7). We subsequently explored the light-triggered transfer of drug/reporter from the lipophilic plasma membrane of erythrocytes to the aqueous milieu. First, exposure of erythrocytes to **C_{18}-Cbl-TAM** revealed even and extensive loading as assessed by widefield fluorescence microscopy. In addition, given the established photolytic sensitivity of the Co-C bond,[6, 8,9] we were not surprised to find that imaging **C_{18}-Cbl-TAM** on erythrocytes results in the rapid migration (<1 s) of TAM fluorescence from erythrocytes into solution (SI Figure S8).

C_{18}-Cbl-MTX, **C_{18}-Cbl-COL** and **C_{18}-Cbl-DEX** were loaded onto intact human erythrocytes with minimal lysis (~5% at 5 μM C_{18}-Cbl-Drug, SI Figure S9). 0.3 – 1.0 fmol of C_{18}-Cbl-Drug loaded per red blood cell. Subsequent photo-release of the drug was quantitative for **C_{18}-Cbl-COL** and **C_{18}-Cbl-DEX** and 35% for **C_{18}-Cbl-MTX** (SI Figure S10):

C_{18}-Cbl-MTX: LC-MS analysis revealed that photolysis of erythrocyte-anchored **C_{18}-Cbl-MTX** primarily furnishes N-propylamide MTX (Figure 3, SI Scheme 11 and Tables S4 – S6). Consistent with the established structure activity relationship of MTX derivatives,[10] the photolyzed product of **C_{18}-Cbl-MTX** serves as an effective inhibitor of dihydrofolate reductase (DHFR, SI Figure S11). In addition, photo-released MTX from erythrocyte-anchored **C_{18}-Cbl-MTX** binds to DHFR in HeLa cells (SI Figure S12).

C_{18}-Cbl-COL: N-butanoyl COL is the primary photoproduct of **C_{18}-Cbl-COL**-loaded erythrocytes (Figure 3 and SI Tables S4 – S6). Photolyzed **C_{18}-Cbl-COL** disrupts microtubules in HeLa cells as effectively as COL itself (SI Figures S13 – S14).

C_{18}-Cbl-DEX: DEX is the observed product from photolysis of **C_{18}-Cbl-DEX**-loaded erythrocytes, instead of one or more of the expected photoproducts (Figure 3 and SI Tables S4 – S6). The 21-esters of DEX are pro-drugs that are hydrolyzed to DEX *in vivo*.[11] The possible presence of blood esterases[12] may explain the formation of DEX once freed from the RBC surface. Photo-release of DEX from **C_{18}-Cbl-DEX**-loaded erythrocytes co-cultured with HeLa cells results in the migration of glucocorticoid receptor α (GRα) from the cytosol to the nucleus in HeLa cells [SI Figures S15 – S16]. We note that, in the absence of illumination, **C_{18}-Cbl-MTX**-, **C_{18}-Cbl-COL**-, and **C_{18}-Cbl-DEX**-loaded erythrocytes do not release their therapeutic contents (SI Figures S12, S14, S16).

We also examined whether C_{18}-Cbl-drugs transfer from erythrocytes to HeLa cells in the absence of light. HeLa cells were incubated with **C_{18}-Cbl-DEX**-loaded erythrocytes and, subsequently, the adherent HeLa cells were washed to remove the red blood cells. If **C_{18}-Cbl-DEX** had migrated to HeLa membranes during the incubation process, illumination at 525 nm should result in DEX release, uptake, and GRα migration. However, we did not observe receptor relocation to the nucleus, suggesting that **C_{18}-Cbl-DEX** is retained by erythrocytes in the dark (SI Figure S17).

With the biological efficacy of the light triggered release of drugs from erythrocytes established, we turned our attention to the assembly of photo-responsive constructs that (1) operate within the optical window of tissue and (2) are encoded to respond to specific wavelengths. Our choice of anti-inflammatory drugs is based upon their role in the treatment of rheumatoid arthritis (RA). The long-term administration of anti-inflammatory agents produce moderate to severe side effects, such as weight gain, osteoporosis, diabetes mellitus, hypertension, skin fragility and infections arising from being systemically immunocompromised.[13–14] Not surprisingly, there is significant interest in the development of therapeutics that can be selectively delivered to RA joints.[15] With this in mind, we prepared C_{18} derivatives of Cy5 (C_{18}-Cy5; λ_{ex} 646 nm), Alexa Fluor 700 (C_{18}-AF700; λ_{ex} 700 nm), Cy7 (C_{18}-Cy7; λ_{ex} 747 nm), and a DyLight 800 analog (C_{18}-DY800;

λ_{ex} 784 nm) and examined whether they are capable of serving as long wavelength antennas for drug release. Photolysis experiments employed in-house constructed LED circuit boards centered at 660 nm (Cy5), 725 nm (AF700 and Cy7), and 780 nm (DY800) (SI Figure S18 and Table S7).

Our initial studies employed **C_{18}-Cbl-TAM** in the presence of the C_{18}-fluorophores, since the photo-release of TAM from **C_{18}-Cbl-TAM**-labelled erythrocytes is readily monitored by fluorescence. In order to identify optimal energy transfer conditions, we first exposed erythrocytes to various relative concentrations of **C_{18}-Cbl-TAM** and **C_{18}-Cy5**. After washing the erythrocytes to remove any unbound **C_{18}-Cbl-TAM** and **C_{18}-Cy5**, the loaded RBCs were illuminated at 660 nm. The carrier erythrocytes were subsequently pelleted via centrifugation and TAM fluorescence in the supernatant measured. Although the most efficient TAM release was observed with erythrocytes exposed to a 1 μM:10 μM of **C_{18}-Cbl-TAM**:**C_{18}-Cy5** (SI Figure S19), we employed a 1 μM:5 μM ratio to keep disruption of the erythrocyte's structural integrity at an absolute minimum. In addition to the **C_{18}-Cy5** @ 660 nm antenna, the photo-release of TAM from **C_{18}-Cbl-TAM**-loaded erythrocytes can be triggered at longer wavelengths in the presence of other antennas [**C_{18}-Cy7** @ 725 nm, **C_{18}-Cy7** @ 725 nm, **C_{18}-DY800** @780 nm]. Figure 4 compares the fraction of TAM released as a function of (a) antenna wavelength, (b) power of the different LEDs, and (c) photon density. An analogous set of experiments with similar results was performed with **C_{18}-Cbl-FAM**/C_{18}-fluorophores (SI Figure S20). Erythrocytes in the dark do not release TAM or FAM and, erythrocytes lacking a fluorophore antenna do not release FAM or TAM at wavelengths longer than those absorbed by Cbl (SI Figures S21 – S23). Finally, confocal microscopy revealed that the structural integrity of erythrocytes is not altered by the addition of the C_{18}-fluorophores (SI Figure S24).

We subsequently examined drug photo-release from the erythrocyte-assembled drug/antenna array. **C_{18}-Cbl-MTX**, **C_{18}-Cbl-COL**, and **C_{18}-Cbl-DEX** were each paired with C_{18}-fluorophores and illuminated. LC-MS confirmed the release of MTX, COL, and DEX at the wavelength absorbed by the partner C_{18}-fluorophore (SI Figures S25 – S26 and Table S8):

C_{18}-Cbl-DEX*/*C_{18}-Cy5: DEX is released from **C_{18}-Cbl-DEX**/**C_{18}-Cy5**-loaded erythrocytes in culture with HeLa cells upon 660 nm exposure. As a consequence, GRα in HeLa cells migrates from the cytoplasm to the nucleus (Figure 5a–b). By contrast, **C_{18}-Cbl-DEX** loaded erythrocytes lacking a long wavelength absorbing antenna fail to trigger GRα migration when exposed to long wavelengths (e.g. 780 nm; SI Figures S27 – S28).

C_{18}-Cbl-COL*/*C_{18}-DY800: 780 nm elicits COL release from erythrocyte-anchored **C_{18}-Cbl-COL**/**C_{18}-DY800**, which induces microtubule depolymerization in the plated HeLa cells (Figure 5c–d, SI Figure S29).

C_{18}-Cbl-MTX*/*C_{18}-Cy7: MTX is released from **C_{18}-Cbl-MTX**/**C_{18}-Cy7**-loaded erythrocytes upon 725 nm exposure. The MTX photo-product associates with endogenous DHFR in the co-cultured HeLa cells as assessed by the cellular thermal shift assay (Figure 5e).[16]

In summary, we've described the cell-mediated assembly of photo-responsive drug release constructs. Release is triggered upon exposure to far-red and near-IR light that falls well within the optical window of tissue. Furthermore, drug release is wavelength-encodable; enabling the action wavelength to be chosen in advance based upon the known excitation properties of a given fluorophore. Finally, although this study focused on erythrocytes as drug carriers, the strategy described herein should prove applicable to nanoparticle drug carriers as well.[17]

Supplementary Material

Refer to Web version on PubMed Central for supplementary material.

Acknowledgments

We thank the NIH for financial support (R01 CA79954)

References

1. Celli JP, Spring BQ, Rizvi I, Evans CL, Samkoe KS, Verma S, Pogue BW, Hasan T. Chem. Rev. 2010; 110:2795–2838. [PubMed: 20353192]
2. Tromberg BJ, Shah N, Lanning R, Cerussi A, Espinoza J, Pham T, Svaasand L, Butler J. Neoplasia. 2000; 2:26–40. [PubMed: 10933066]
3. (a) Lee HM, Larson DR, Lawrence DS. ACS Chem. Biol. 2009; 4:409–427. [PubMed: 19298086] (b) Klan P, Solomek T, Bochet CG, Blanc A, Givens R, Rubina M, Popik V, Kostikov A, Wirz J. Chem. Rev. 2013; 113:119–191. [PubMed: 23256727]
4. Bort G, Gallavardin T, Ogden D, Dalko PI. Angew. Chem. Int. Ed. Engl. 2013; 52:4526–4537. [PubMed: 23417981]
5. Chen G, Qiu H, Prasad PN, Chen, X X. Chem. Rev. 2014; 114:1236–1250.
6. Shell TA, Shell JR, Rodgers ZL, Lawrence DS. Angew. Chem. Int. Ed. 2014; 53:875–878.
7. Muzykantov VR. Expert Opin. Drug Deliv. 2010; 7:403–427. [PubMed: 20192900]
8. (a) Dolphin D, Johnson AW, Rodrigo, R R. Ann. N Y Acad. Sci. 1964; 112:590–600. [PubMed: 14167292] (b) Taylor RT, Smucker L, Hanna ML, Gill J. Arch Biochem Biophys. 1973; 156:521–533. [PubMed: 4718782] (c) Halpern J, Kim S-H, Leung TW. J. Am. Chem. Soc. 1984; 106:8317–8319.(d) Kozlowski PM, Kumar M, Piecuch P, Li W, Bauman NP, Hansen JA, Lodowski P, Jaworska M. J. Chem. Theory Comp. 2012; 8:1870–1894.
9. Priestman MA, Shell TA, Sun L, Lee HM, Lawrence DS. Angew. Chem. Int. Ed. 2012; 51:7684–7687.
10. (a) McGuire JJ. Cur. Pharm. Design. 2003; 9:2593–2613.(b) Antonjuk DJ, Boadle DK, Cheung HTA, Friedlander ML, Gregory PM, Tattersall MHN. Arzneimittel-Forschung. 1989; 39:12–15. [PubMed: 2719739]
11. (a) Markovic BD, Vladimirov SM, Cudina OA, Odovic JV, Karljikovic-Rajic KD. Molecules. 2012; 17:480–491. [PubMed: 22222907] (b) Civiale C, Bucaria F, Piazza S, Peri O, Miano F, Enea V. J. Ocul. Pharmacol. Ther. 2004; 20:75–84. [PubMed: 15006161]
12. Richter D, Croft PG. Biochem. J. 1942; 36:746–757. [PubMed: 16747503]
13. Huscher D, Thiele K, Gromnica-Ihle E, Hein G, Demary W, Dreher R, Zink A, Buttgereit F. Ann. Rheum. Dis. 2009; 68:1119–1124. [PubMed: 18684744]
14. Baschant U, Lane NE, Tuckermann J. Nat. Rev. Rheumatol. 2012; 8:645–655. [PubMed: 23045254]
15. (a) Mitragotri S, Yoo JW. Arch. Pharm. Res. 2011; 34:1887–1897. [PubMed: 22139688] (b) Fiehn C. Clin. Exp. Rheumatol. 2010; 28:S40–S45. [PubMed: 21044432] (c) Ulbrich W, Lamprecht A. J. R. Soc. Interface. 2010; 7(Suppl 1):S55–S66. [PubMed: 19940000]

16. Molina DM, Jafari R, Ignatushchenko M, Seki T, Larsson EA, Dan C, Sreekumar L, Cao Y, Nordlund P. Science. 2013; 341:84–87. [PubMed: 23828940]

17. (a) Puri A. Pharmaceutics. 2013; 6:1–25. [PubMed: 24662363] (b) Tong R, Kohane DS. Wiley Interdiscip. Rev. Nanomed. Nanobiotechnol. 2012; 4:638–662. [PubMed: 22887840] (c) Alvarez-Lorenzo C, Bromberg L, Concheiro A. Photochem. Photobiol. 2009; 85:848–860. [PubMed: 19222790]

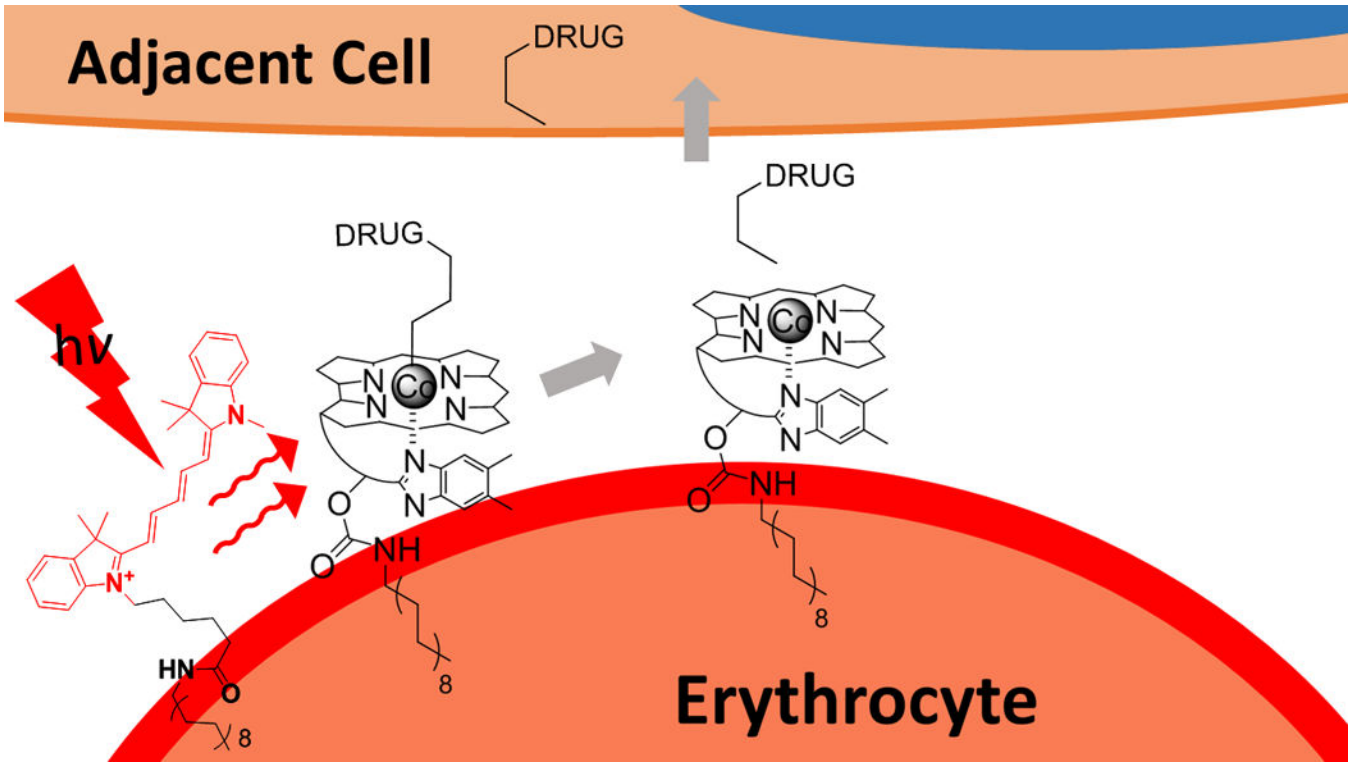

Figure 1.

A wavelength-encoded drug release strategy. Anti-inflammatory drugs are covalently appended to Cbl via a photolabile Co-C bond. Lipidated-Cbl and -fluorophore constructs assemble on the plasma membrane of human erythrocytes. The fluorophore serves as an antenna, capturing long wavelength light and transmitting the energy to the Cbl-drug, resulting in drug release from the erythrocyte carrier.

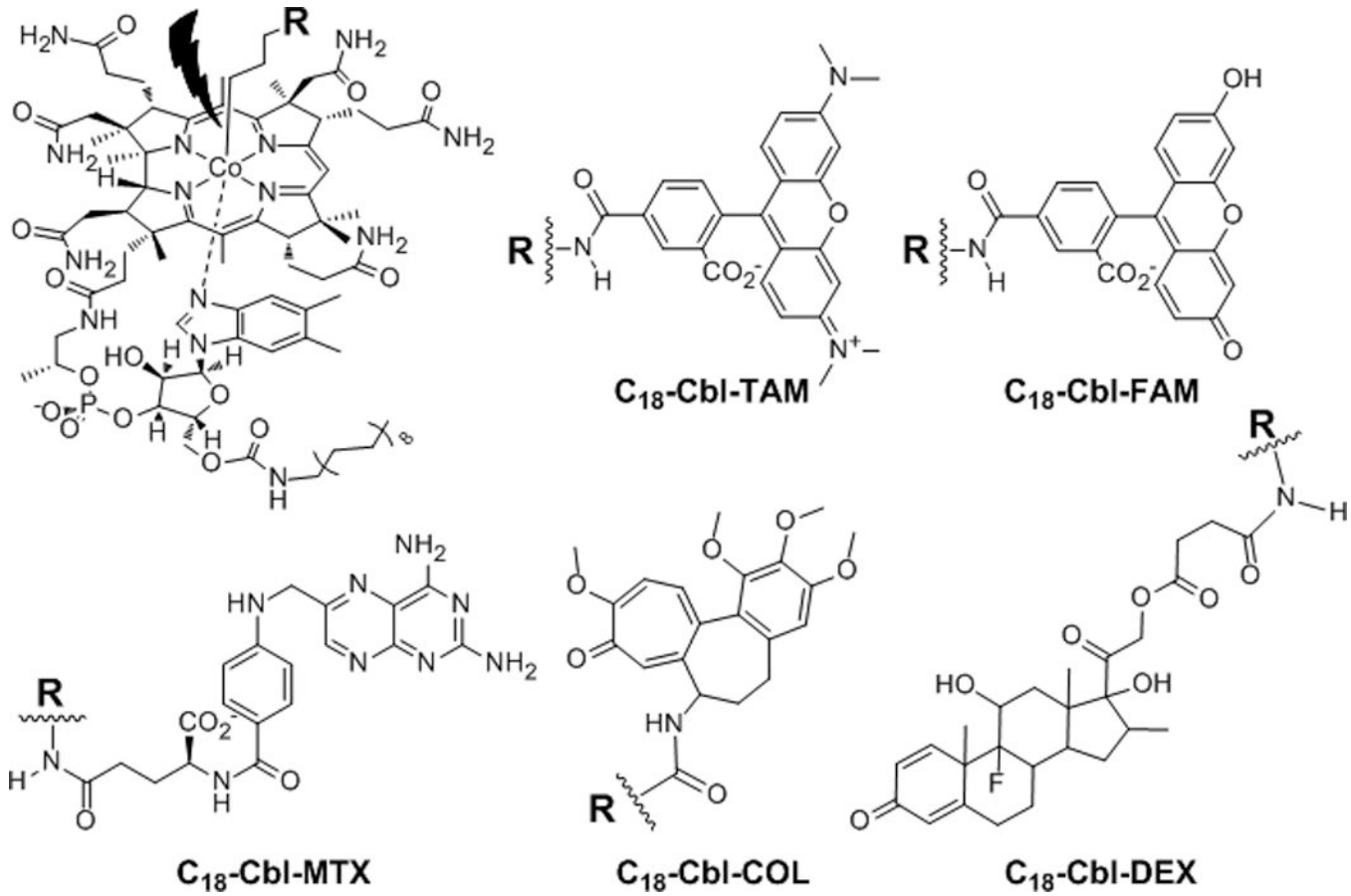

Figure 2.

Anti-inflammatory drugs are Lipidated Cbl-reporters, TAM (**C_{18}-Cbl-TAM**) and FAM (**C_{18}-Cbl-FAM**) and lipidated Cbl-drug conjugates, MTX (**C_{18}-Cbl-MTX**), COL (**C_{18}-Cbl-COL**), and DEX (**C_{18}-Cbl-DEX**).

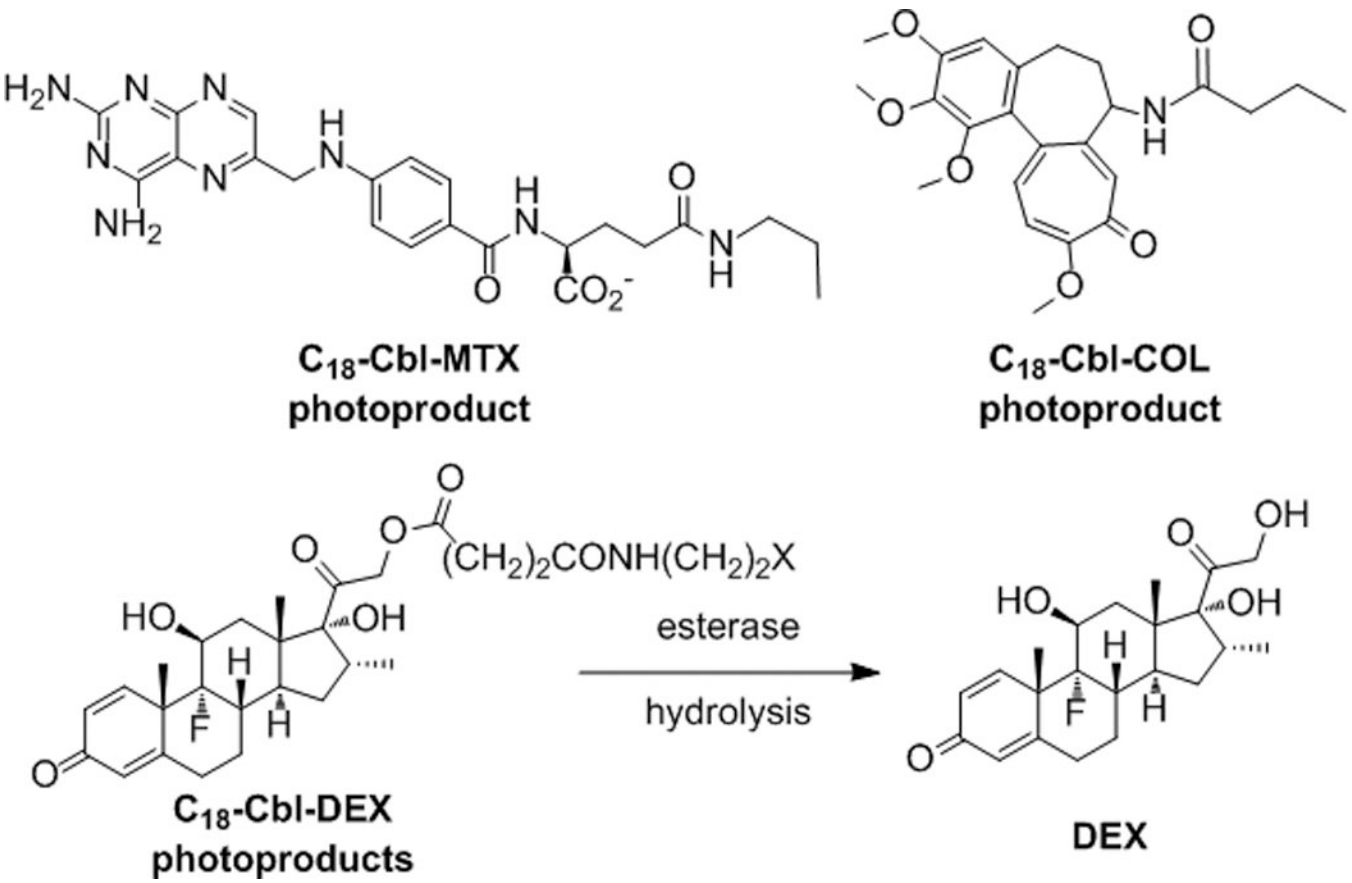

Figure 3.

Erythrocyte-released photoproducts of **C_{18}-Cbl-MTX**, **C_{18}-Cbl-COL** and **C_{18}-Cbl-DEX**. In the case of **C_{18}-Cbl-DEX**, DEX is observed, instead of the possible photoproducts (X = H, OH, or =O).

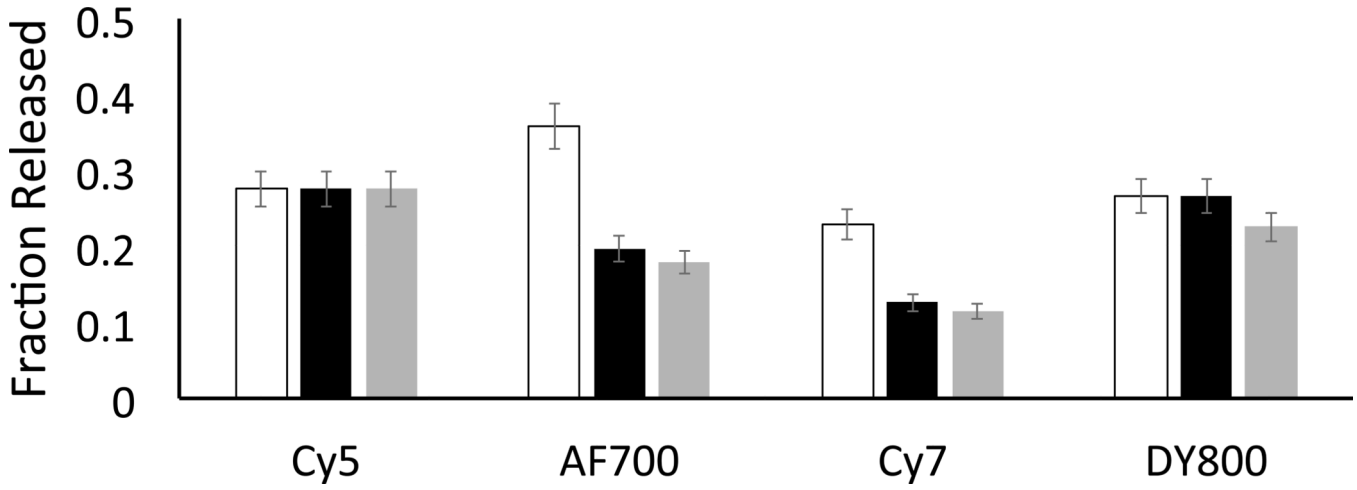

Figure 4.

Photo-release of TAM from **C_{18}-Cbl-TAM**/C_{18}-fluorophore-loaded erythrocytes. LED arrays centered at 660 nm (Cy5), 725 nm (AF700 and Cy7), and 780 nm (DY800) were employed as the light sources. TAM release is displayed as the fraction liberated from erythrocytes. Total erythrocyte bound **C_{18}-Cbl-TAM** was determined via a time study where 3 h of illumination generated maximal TAM release. Unfilled bars: fraction of TAM release; Black bars: fraction of TAM release normalized by the power of the different light sources; Grey bars: fraction of TAM release normalized by photon density produced by the light sources; n = 3 for all experiments. See the legend to SI Figure 20 for an explanation of the normalizations.

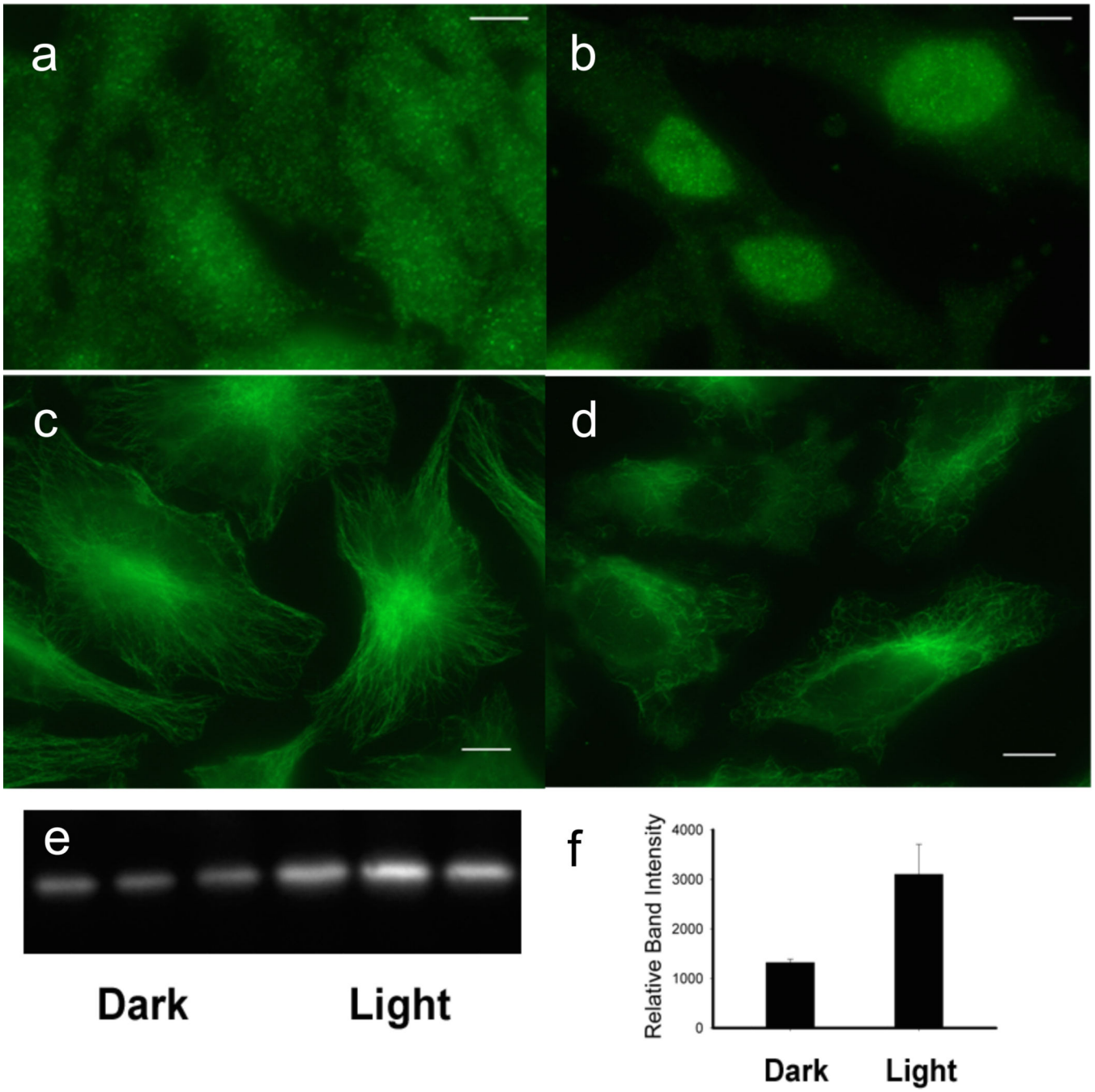

Figure 5.

Release of anti-inflammatory agents from erythrocytes and their affect on HeLa cells. (a) – (b) DEX release from **C_{18}-Cbl-DEX/C_{18}-Cy5**-loaded erythrocytes at 660 nm triggers HeLa cell GRα nuclear localization, where (a) is dark and (b) 660 nm. HeLa GRα visualized with Alexa488 antiRabbit/anti-GRα. (c) – (d) COL release from **Cbl-COL/C_{18}-DY800** erythrocytes at 780 nm initiates HeLa microtubule depolymerization, where (c) is dark and (d) 780 nm. HeLa microtubules visualized with Alexa488 antiMouse/anti-tubulin. Bar = 5 μm. (e) – (f) MTX release from **C_{18}-Cbl-MTX/C_{18}-Cy7**-loaded erythrocytes at 725 nm

shifts the thermal stability of DHFR where left 3 lanes (dark) and right 3 lanes (725 nm). GAPDH used as loading control (SI Figure S30).